Journal of Visualized Experiments

Preparation of Multifunctional Silk-Based Microcapsules Loaded with DNA Plasmids Encoding RNA Aptamers and Riboswitches

--Manuscript Draft--

Article Type:	Invited Methods Collection - JoVE Produced Video
Manuscript Number:	JoVE62854R2
Full Title:	Preparation of Multifunctional Silk-Based Microcapsules Loaded with DNA Plasmids Encoding RNA Aptamers and Riboswitches
Corresponding Author:	Irina Drachuk, Ph.D. AFRL: Air Force Research Laboratory Wright Patterson AFB, OH UNITED STATES
Corresponding Author's Institution:	AFRL: Air Force Research Laboratory
Corresponding Author E-Mail:	idrachuk@ues.com
Order of Authors:	Irina Drachuk, Ph.D.
	Svetlana Harbaugh
	Nancy Kelley-Loughnane
	Jorge L. Chávez
Additional Information:	
Question	**Response**
Please specify the section of the submitted manuscript.	Biology
Please indicate whether this article will be Standard Access or Open Access.	Standard Access ($1400)
Please indicate the **city, state/province, and country** where this article will be **filmed**. Please do not use abbreviations.	AFRL, Dayton, OH 45432
Please confirm that you have read and agree to the terms and conditions of the author license agreement that applies below:	I agree to the Author License Agreement
Please provide any comments to the journal here.	Dear Editor, we addressed the comments according to the remarks. Please, let us know if there are any concerns that might delay the production of the manuscript. Thank you.
Please confirm that you have read and agree to the terms and conditions of the video release that applies below:	I agree to the Video Release

TITLE:

Preparation of Multifunctional Silk-Based Microcapsules Loaded with DNA Plasmids Encoding RNA Aptamers and Riboswitches

AUTHORS AND AFFILIATIONS:

Irina Drachuk[1,2], Svetlana Harbaugh[2], Nancy Kelley-Loughnane[3], Jorge L. Chávez[2]

[1]UES Inc., Dayton, OH 45432, US.

[2]711th Human Performance Wing, Airman Systems Directorate, Air Force Research Laboratory, Wright-Patterson AFB, OH 45433, US.

[3]Materials and Manufacturing Directorate, Air Force Research Laboratory, Wright-Patterson AFB, OH 45433, US.

Email addresses of co-authors:

Irina Drachuk	(irina.drachuk.ctr@us.af.mil)
Svetlana Harbaugh	(svetlana.harbaugh.4@us.af.mil)
Nancy Kelley-Loughnane	(nancy.kelley-loughnane.1@us.af.mil)
Jorge L. Chávez	(jorge.chavez_benavides.2@us.af.mil)

Corresponding authors:

Irina Drachuk	(irina.drachuk.ctr@us.af.mil)
Jorge. L. Chávez	(jorge.chavez_benavides.2@us.af.mil)

SUMMARY:

The protocol describes the formation of robust and biocompatible DNA-laden microcapsules as multiplexed *in vitro* biosensors capable of tracking several ligands.

ABSTRACT:

We introduce a protocol for the preparation of DNA-laden silk fibroin microcapsules via the Layer-by-Layer (LbL) assembly method on sacrificial spherical cores. Following adsorption of a prime layer and DNA plasmids, the formation of robust microcapsules was facilitated by inducing β-sheets in silk secondary structure during acute dehydration of a single silk layer. Hence, the layering occurred via multiple hydrogen bonding and hydrophobic interactions. Upon adsorption of multilayered shells, the core-shell structures can be further functionalized with gold nanoparticles (AuNPs) and/or antibodies (IgG) to be used for remote sensing and/or targeted delivery. Adjusting several key parameters during sequential deposition of key macromolecules on silica cores such as the presence of a polymer primer, the concentration of DNA and silk protein, as well as a number of adsorbed layers resulted in biocompatible, DNA-laden microcapsules with variable permeability and DNA loadings. Upon dissolution of silica cores, the protocol demonstrated the formation of hollow and robust microcapsules with DNA plasmids immobilized to the inner surface of the capsule membrane. Creating a selectively permeable biocompatible membrane between the DNA plasmids and the external environment preserved the DNA during long-term storage and played an important role in the improved output response from spatially confined plasmids. The activity of DNA templates and their accessibility were

tested during *in vitro* transcription and translation reactions (cell-free systems). DNA plasmids encoding RNA light-up aptamers and riboswitches were successfully activated with corresponding analytes, as was visualized during localization of fluorescently labeled RNA transcripts or GFPa1 protein in the shell membranes.

INTRODUCTION:

The field of synthetic biology offers unique opportunities to develop sensing capabilities by exploiting natural mechanisms evolved by microorganisms to monitor their environment and potential threats. Importantly, these sensing mechanisms are typically linked to a response that protects these microorganisms from harmful exposure, regulating gene expression to mitigate negative effects or prevent intake of toxic materials. There have been significant efforts to engineer these microorganisms to create whole-cell sensors taking advantage of these natural responses but re-directing them to recognize novel targets and/or to produce a measurable signal that can be measured for quantification purposes (typically fluorescence)[1,2]. Currently, concerns with the use of genetically modified microorganisms (GMOs), especially when releasing in the environment or the human body, due to leakage of whole cells or some of their genetic material, even if encapsulated in a polymer matrix, suggest that alternative ways to exploit these sensing approaches are needed[3].

A powerful approach to exploit the benefits of microorganisms-based sensing without the concern for the deployment of GMOs is the use of *in vitro* transcription/translation (IVTT) systems. From a practical perspective, IVTT systems consist of a mixture containing most of the cell components in an active state that has been "extracted" from cells by different means, including sonication, bead-beating, or others[4]. The final product of this process is a biochemical reaction mixture already optimized to perform transcription and translation that can be used to test different sensors in an "open vessel" format, without the constraints associated with the use of whole cells (membrane diffusion, transformation efficiency, cell toxicity, etc.). Importantly, different sensor components can be quantitatively added, and their effect studied by different optical and spectrometric techniques, as we have demonstrated[5]. It has been noticed that the performance of IVTT systems can be inconsistent; however, recent studies have shown approaches to standardize their preparation and characterization, which is of great help when studying their performance in sensor design[6]. Recently, many examples of IVTT systems using to create paper-based assays through the lyophilization of their components in paper matrices have been demonstrated, including detection of heavy metal ions, drugs, quorum sensing elements, and others[7–9]. An exciting application space for IVTT-based sensors is their use in sensing applications in different types of environments, including soil, water, and the human body. In order to deploy these IVTT systems to these challenging environments, an encapsulation approach need to be implemented to contain the IVTT components and protect them from degradation.

The most common encapsulation approaches for IVTT systems include the use of lipid capsules, micelles, polymersomes, and other tightly enclosed microcontainers[10–12]. One disadvantage of this approach is the need to incorporate either passive or active mechanisms to transport materials in and out of the containers to allow communication with the external environment

and provide sensing capabilities. To overcome some of these issues, the study here reports a method that provides a simple yet effective approach to encapsulate the encoding materials for different sensor designs to be expressed in IVTT systems. This approach is based on the use of Layer-by-Layer (LbL) deposition of a biopolymer in the presence of the plasmids of interest to create hollow microcapsules with high porosity, which allows the protected genetic material to interact with the different components of the IVTT of choice. The study demonstrated that encapsulated plasmids could direct transcription and translation when activated within this polymeric matrix, as shown with the response of a plasmid-encoded aptamer and a riboswitch to their corresponding targets. Additionally, this LbL coating protects the plasmids for months without any special storage conditions**.**

PROTOCOL:

1. Construction of plasmid vector.

1.1. Construct a plasmid vector (pSALv-RS-GFPa1, 3.4 kb) by amplification of the coding sequence of a theophylline riboswitch (ThyRS) coupled with GFPa1 from pJ201:23976-RS-GFPa1 vector (designed and created by DNA2.0) and insertion into *E. coli* expression vector, pSAL[13]. Use forward (5'-CGTGGTACCGGTGATACCAGCATCGTCTTGATG-3') and reverse (5'-CGTGCTCAGCTTAAGCCAGCTCGTAG-3') primers to amplify the coding sequence of ThyRS coupled with GFPa1 and perform a PCR reaction in 50 µL volume using DNA polymerase according to the manufacturer's protocol[14].

1.2. Prepare a 1% agarose gel from 0.5 g of agarose, 50 mL of TAE buffer (40 mM Tris Acetate, 1 mM EDTA, pH 8.0), and 3 µL of DNA stain.

1.3. Mix 5 µL aliquot of the PCR-amplified product with 5 µL of RNase/DNase-free water and 2 µL of 6x gel loading dye and analyze by agarose gel electrophoresis. Load a DNA ladder (0.1–10.0 kb) as a reference. Run the gel at 120 V until the dye line has almost reached the bottom of the gel.

1.4. Visualize the DNA fragments using a UV transilluminator imaging system to check for the correct size of DNA[15].

1.5. Purify the PCR product using a PCR purification kit according to the manufacturer's protocol[16].

1.6. Digest the PCR product and pSAL expression vector with KpnI and BlpI restriction enzymes in a 15 µL reaction, containing 10 µL of PCR product or plasmid vector (concentration 20–50 ng/µL), 1.5 µL of 10x enzyme buffer, 1 µL of each enzyme, and 1.5 µL of RNase/DNase-free water, at 37 °C for 2 h.

1.7. Add 3 µL of 6x gel loading dye to the reaction mixture and separate the digested fragments on a 1% agarose gel as described in steps 1.3–1.5.

1.8. Purify the DNA fragments using a gel extraction kit according to the manufacturer's protocol[16].

1.9. Ligate the digested PCR product into a digested linearized plasmid vector, pSAL, using T4 DNA ligase and supplemented ligase buffer in a 10 µL reaction containing 3–20 fmol of the digested vector, 9–60 fmol of the digested PCR product, 2 µL of ligase buffer, 1 µL (1 unit) of T4 DNA Ligase, and DNase/RNase-free water. Incubate the ligation reaction at 25 °C for 3 h.

NOTE: Ensure that the total DNA content in the reaction mixture is 0.01–0.1 µg.

1.10. Transform *E. coli* DH5α competent cells with 10 ng of the ligation reaction mixture according to the manufacturer's protocol[17].

1.11. Grow the transformed cells at 37 °C overnight on LB-agar plates supplemented with ampicillin (100 µg/mL).

1.12. Pick 3–4 bacterial colonies from the plate and aseptically transfer each of them into 5 mL of LB media supplemented with ampicillin (100 µg/mL). Grow the cultures overnight at 37 °C in a shaking incubator at 225 rpm.

1.13. Pellet the overnight cultures by centrifugation at 11 x *g* for 3 min at room temperature.

1.14. Use a purification kit to purify the plasmids according to the manufacturer's protocol[16].

1.15. Verify the sequences of the purified plasmids by DNA sequencing. The plasmid map and the sequence of the resulting construct (pSALv-RS-GFPa1) are shown in **Figure 1**.

2. Large-scale DNA purification.

2.1. Transform the plasmid vector pSALv-RS-GFPa1 (3.4 kb) (encoding theophylline riboswitch coupled with GFPa1 reporter gene) or pET28c-F30-2xBroccoli (5.4 kb) (encoding Broccoli aptamer) into *E. coli* DH5α competent cells according to the manufacturer's protocol[17].

2.2. Grow the transformed cells at 37 °C overnight on LB-agar plates supplemented with ampicillin (100 µg/mL) for cells transformed with pSALv-RS-GFPa1 or kanamycin (50 µg/mL) for cells transformed with pET28c-F30-2x Broccoli.

2.3. Pick 3–4 bacterial colonies from the plate and aseptically transfer each colony into 5 mL of LB media supplemented with appropriate antibiotic (100 µg/mL ampicillin or 50 µg/mL kanamycin). Grow the cultures overnight at 37 °C in a shaking incubator at 225 rpm.

2.4. Use 3 mL of the overnight culture to inoculate into 150 mL of LB supplemented with appropriate antibiotic (100 µg/mL ampicillin or 50 µg/mL kanamycin) and grow the cultures

overnight at 37 °C in a shaking incubator at 225 rpm.

2.5. Pellet the cells by centrifugation at ≥3400 x *g* for 10 min at 4 °C.

2.6. Use a purification kit to purify the plasmids according to the manufacturer's protocol[16].

2.7. Elute the DNA with 0.5 mL of pure DNase/RNase-free water. Measure the DNA concentration and prepare 1 mL of DNA stock solutions (100 ng/µL). Store the tubes with DNA at 4 °C until further use.

3. Extraction of silk fibroin and preparation of initial materials.

3.1. Prepare an aqueous solution of reconstituted silk fibroin (SF) protein from *Bombyx mori* silkworm cocoons according to the procedure described in detail elsewhere to account for 10% of Silk-LiBr solution[18].

3.2. Determine the final concentration of the aqueous SF solution. Pipette 0.5 mL of silk solution to a 60 mm Petri dish, let it dry at 60 °C, and measure the weight of dry silk film. Divide the dry weight by 0.5 mL to calculate the weight per volume percentage.

3.3. Dilute the concentrated silk solution with DNase/RNase-free distilled water by slowly adding water via serological pipette to obtain 1 mg/mL final concentration. Store the solution at 4 °C for future use.

3.4. Prepare fluorescently labeled silk fibroin using an antibody labeling kit. Use 1 mL of 2 mg/mL silk fibroin solution to couple the N-terminal α-amino groups of the protein with an NHS ester-activated derivative dye according to the manufacturer's protocol[19].

3.5. Prepare 50 mL of polyethyleneimine (PEI) aqueous solution with a concentration of 6 mg/mL, adjust pH to 4 with HCl (1 M). Filter the solution through a sterile 0.2 µm membrane. Storage is possible at ambient conditions for months.

3.6. Prepare SiO_2 cores. Pipette 300 µL of SiO_2 particles into a 2 mL microcentrifuge tube. Wash the microparticles two times with 1 mL of DNase/RNase-free water by centrifugation at 0.2 x *g* for 1 min.

4. Perform Layer-by-Layer deposition of a prime layer, DNA plasmids, and silk layers.

4.1. To deposit the PEI prime layer onto the SiO_2 microparticles, add 1 mL of PEI solution to the spun down pellet from step 3.6 and agitate the mixture at ambient conditions on a thermomixer at 800 rpm for 15 min. Wash the particles four times with 1 mL of DNase/RNase-free deionized water by centrifugation at 0.2 x *g* for 1 min.

4.2. To perform deposition of the DNA layer, add 1 mL of the aqueous solution of DNA

plasmids from step 2.7 to the PEI-primed microparticles and gently agitate the mixture at 4 °C on a thermomixer at 800 rpm for 15 min. To prepare microcapsules with different DNA loads, adjust the concentration of DNA plasmids from 50–200 ng/µL using DNase/RNase-free distilled water and use 1 mL of these solutions to deposit the DNA. Collect the microparticles by centrifugation at 0.2 x *g* for 1 min.

4.3. Mark the tubes for DNA plasmids encoding theophylline riboswitch coupled with GFPa1 as ThyRS-GFPa1, and DNA plasmids encoding Broccoli aptamer as BrocApt.

NOTE: Keep the microcentrifuge tubes with DNA on ice.

4.4. Carefully remove the supernatant and wash the microparticles four times with 1 mL of DNase/RNase-free distilled water, each time discarding the supernatant after centrifugation at 0.2 x *g* for 1 min. Perform all experiments at room temperature (RT) unless it is specified otherwise.

4.5. To perform deposition of the silk fibroin layer add 1 mL of the reconstituted aqueous SF solution from step 3.3 to the DNA-adsorbed microparticles, gently vortex and agitate the mixture at 10 °C on the thermomixer at 750 rpm for 15 min. Collect the microparticles by centrifugation at 0.2 x *g* for 1 min at 4 °C, remove the supernatant, and then wash them once with 1 mL of DNase/RNase-free distilled water. Repeat the centrifugation and discard the supernatant.

NOTE: During the experiment, keep the solution of silk on ice to avoid temperature-induced gelation.

4.6. Gradually treat the particles with methanol to induce β-sheet formation in silk protein structure. First, add 0.5 mL of DNase/RNase distilled water, vortex the microcentrifuge tube, then add 0.5 mL of 100% methanol. Gently shake the particles on the thermomixer at 10 °C for 5 min. Collect the particles by centrifugation at 0.2 x *g* for 1 min. Remove the supernatant.

4.7. Treat the particles with methanol to promote the formation of β-sheets and ensure strong physical adsorption of the silk layer. Add 1 mL of 100% methanol. Gently shake the particles on the thermomixer at 750 rpm for 10 min at 10 °C.

4.8. Collect the particles by centrifugation at 0.2 x *g* for 1 min at 4 °C and wash them twice with 1 mL of DNase/RNase-free distilled water each time, discarding the supernatant and gently vortexing before the next centrifugation.

4.9. Repeat steps 4.5–4.8 20 times to obtain silk multilayered core-shell structures. For the last deposition step, use fluorescently labeled silk from step 3.4 (Silk-DyLight550, 1 mL).

4.10. Perform the last washing step and keep the microparticles in 1 mL of DNase/RNase-free distilled water at ambient conditions.

NOTE: To avoid aggregation of particles during deposition of silk layers, perform a visual inspection of the particles suspension and pipette it up and down using a 1 mL pipette tip to promote homogeneous particle distribution.

4.11. Calculate the number of DNA plasmid copies encapsulated in each microcapsule, N_{DNA} using Equation 1:

$$N_{DNA} = \frac{(C \times V)/N \times 0.8}{M_w} \times N_A \qquad (1)$$

Where $N = 6.769 \times 10^{11}$ – the number of SiO_2 cores used for encapsulation. Calculate it from a standard curve for known concentrations of silica particles using serial dilutions and absorption A_{320} at $\lambda = 320$ nm;

C – initial concentration of DNA used for adsorption
V – the volume of DNA used for adsorption
0.8 – DNA adsorption efficiency on the cores
M_w – Molecular weight of DNA plasmid
N_A – Avogadro's number (6.022×10^{23})

5. Dissolution of cores to obtain silk microcapsules.

5.1. Prepare 8% hydrofluoric acid (HF) solution, pH 5.5, by diluting stock solution (48%) with distilled water. Acquire a 50 mL centrifuge tube. Carefully pipette 5 mL of HF and add 25 mL of distilled water to obtain 8% HF solution.

CAUTION: HF is a highly corrosive acid and may cause severe burns to the tissues. Extreme caution must be taken during the handling and use of HF for the experiments. Adhere to Standard Operating Procedure (SOP) for the proper usage and handling of HF developed by the organization to avoid undesirable spillage accidents. Do not use glass containers to dilute HF acid. Use the chemical hood to perform this step of the protocol.

5.2. Dissolve SiO_2 cores by adding 1.5 mL of 8% HF solution to pelleted core-shell microparticles from step 4.10. Gently vortex and let cores dissolve overnight at ambient conditions with gentle shaking at 450 rpm.

NOTE: To avoid spillage of HF, use grafting tape to seal the microcentrifuge tube. Use a chemical hood to perform this step of the protocol.

5.3. Prepare a 2 L glass beaker filled with 2 L of deionized water. Transfer microcapsules solution to dialysis devices (50 kDa MWCO) and dialyze them against deionized water with a repeated change of the water every 3 h for the next 3 days.

NOTE: Collect the supernatant during the first three exchanges of water and discard the solution according to the established protocol for hazardous waste materials.

5.4. Use a 1 mL pipette to transfer the suspension from dialysis devices into new 2 mL microcentrifuge tubes to collect the microcapsules.

NOTE: Store the aqueous solutions of microcapsules at ambient conditions for several years.

6. Imaging of silk fibroin microcapsules using confocal laser scanning microscope (CLSM).

6.1. Perform DNA staining using a DNA dye.

6.1.1. Transfer 300 µL of hollow silk fibroin microcapsules into a fresh 1 mL microcentrifuge tube. Add 500 µL of RNase/DNase-free distilled water.

6.1.2. Add 5 µL of the DNA staining dye, briefly vortex, and incubate at RT for 2 h protected from light.

6.1.3. Perform four washing steps by centrifugation at 0.1 x *g* for 20 min at 4 °C each time, carefully removing 400 µL of the supernatant and replenishing it with 400 µL of RNase/DNase-free distilled water.

6.2. Perform the imaging of silk capsules on inverted confocal systems equipped with three major lasers (405 nm, 488 nm, 561 nm) using 100x oil-immersion objective (NA 1.49). Transfer 100 µL of the capsule sample into a single well of 8-well chambered glass slides, allow for capsules to sediment for 20–30 min prior to imaging.

NOTE: Dyes are very sensitive to photobleaching. Protect the samples by covering the slides with aluminum foil.

7. Estimation of the permeability of hollow microcapsules using molecular weight cut-off (MWCO) method.

7.1. Prepare 2 mL each of FITC-labeled dextran fluorophore solutions (20 µM, diH_2O) of different M_w (4 kDa, 20 kDa, 40 kDa, 70 kDa, 150 kDa, 250 kDa, 500 kDa, and 2 MDa).

7.2. Pipette 100 µL of the suspension of capsules into a single well of a chambered glass slide. Analyze each microcapsule design (concentration of PEI, loading number of DNA plasmids, the concentration of silk fibroin, and the number of layers) separately.

7.3. To each well, add 300 µL of the specific fluorophore solution starting from the lowest M_w up to the highest, so each well will correspond to the specific fluorophore solution. Mix by pipetting up and down and let the mixture incubate for 1 h at RT until the diffusion of fluorophore solutions reaches equilibrium.

7.4. Transfer the slide to a confocal laser scanning microscope (CLSM) and image each well

using 100x oil-immersion objective at excitation λ = 488 nm.

7.4.1. Identify the area of interest by adjusting the focal plane to make sure that the capsules appear in the form of circles of the largest diameter. This typically happens when viewing the samples closer to the bottom of the well when capsules sediment due to gravity.

7.4.2. Collect several images of microcapsule samples by moving the slide in XY direction. Capture images to account for up to 100–150 capsules for each sample.

7.4.3. Use ImageJ software to analyze the permeability of the capsule's membrane in each M_w fluorophore solution by comparing fluorescence intensities inside and outside of the capsules. For that, draw a region of interest (ROI) in the form of a circle to outline the circumference of the capsule and click **Analyze**/**Measure** to measure the fluorescence intensity inside. Tabulate the data into a spreadsheet. Perform this operation for each microcapsule for a total of 200–300 capsules.

7.4.4. Assess the outside fluorescence intensity in the same way by outlining the ROI and measuring the intensity away from the capsules. Perform 3–5 measurements for statistical analysis.

7.4.5. To perform statistical analysis, compare the fluorescence intensities inside and outside of the capsules using paired *t*-test ($p < 0.05$).

7.4.6. Use the conversion **Table 2** to estimate the permeability of microcapsules based on the hydrodynamic radii for FITC-Dextran with variable M_w.

8. *In vitro* activation of synthetic theophylline riboswitch in silk microcapsules

8.1. Prepare 1 mL of theophylline stock solution (100 mM, DMSO). Prepare *E. coli* S30 extract system for circular DNA by thawing the components on ice for 40 min.

8.2. Obtain a 0.5 mL DNase/RNase-free microcentrifuge tube. Perform *in vitro* transcription/translation reaction, combine the cell-free components with a sample of microcapsules in the following order (50 µL total volume): S30 premix without amino acids (20 µL); S30 extract, circular (15 µL); complete amino acids mixture (5 µL); hollow microcapsules containing ThyRS-GFPa1 plasmids from step 4.10 (9 µL); and theophylline, 100 mM DMSO (1 µL).

NOTE: After adding all components, briefly vortex the tube and collect the sample during brief centrifugation at 0.2 × *g* for a couple of seconds.

8.3. Incubate the tube at 30 °C for 4 h and check the fluorescence on a plate reader using excitation at λ = 488 nm and emission for GFP/FITC filter (510 nm ± 20 nm).

8.4. Image the capsules on any LCSM system using 488 nm and 561 nm lasers. Obtain the best

quality images using 100x oil immersion objective and 8-well chambered slides.

9. *In vitro* activation of broccoli aptamer in silk microcapsules

9.1. Prepare 1 mL of stock solution of DFHBI-1T dye (30 µM, diH_2O). Prepare the PURE (protein synthesis using recombinant elements) cell-free system reaction kit by thawing the components on ice for 40 min.

9.2. Obtain a 0.5 mL DNase/RNase-free microcentrifuge tube. Perform *in vitro* transcription reaction by combining cell-free reaction components with a sample of microcapsules in the following order (50 µL total volume): solution A (20 µL); solution B (15 µL); hollow microcapsules containing BrocApt plasmids from step 4.10 (14 µL); and DFHBI-1T dye (1 µL).

NOTE: After adding all components, briefly vortex the tube and collect the sample during brief centrifugation at 0.2 × *g* for a couple of seconds.

9.3. Incubate the tube at 37 °C for 6 h and check the fluorescence on a plate reader using excitation at λ_{ex} = 470 nm and emission at λ_{em} = 510 nm ± 20 nm.

9.4. Image the capsules on any LCSM system using 488 nm and 561 nm lasers. Obtain the best quality images using 100x oil-immersion objective, and 8-well coverglass chambered slides.

REPRESENTATIVE RESULTS:

Here, the study addresses the functionality of DNA templates encoding different sensor designs (two types of RNA-regulated transcription/translation elements) after encapsulation in silk protein capsules. Microcapsules were prepared via templated Layer-by-Layer (LbL) assembly of the key components: A prime layer, DNA plasmids encoding sensor designs, and silk fibroin biopolymer (**Figure 2**). Deposition of macromolecules in a layered fashion allows controlling the permeability of the capsule membrane based on inter- and intramolecular interactions between the absorbed layers and the thickness of the shell. The tunable permeability of the system offered the potential to control the diffusion of essential molecules while limiting the diffusion of large undesirable macromolecules through the capsule membrane[20].

Homogeneous in size (4.5 µm) and robust silk fibroin microcapsules with a shell thickness of ~500 nm (20 layers) in a hydrated state can be produced when properly following the protocol (**Figure 3**)[21]. The LbL approach allowed to tune the loading capacity of DNA templates based on the initial concentration of the plasmids. The optimal DNA loading can be achieved by varying the initial concentration of DNA templates from 50–200 ng/µL. **Table 1** represents the number of DNA copies retained in a single microcapsule upon completion of LbL encapsulation and was calculated for each sensor design based on the initial DNA concentrations and M_w of DNA plasmids according to Equation 1. The optimal DNA loading capacity was achieved with 32 and 20 DNA copies for ThyRS and BrocApt sensor designs, respectively. The assessment of loading capacity was important to have an accurate estimation of the encapsulated DNA concentrations to be able to titrate it during IVTT activation of the sensors by adding more concentrated capsule

samples.

The permeability of the capsule shells can be systematically analyzed by following the MWCO method. The method estimates the pore size of the membrane based on the molecular weight of solute molecules that could not penetrate through the capsule membrane. By subjecting microcapsules to variable M_w fluorophore molecules and performing confocal imaging in the focal plane that corresponds to the largest diameter across multiple capsules, the permeability of the shell membranes can be assessed. ImageJ analysis allows to estimate the fluorescence intensities inside and outside of the capsules and identify fully permeable (outside and inside fluorophore intensities were comparable), partially permeable (50%–70% of capsules had lower fluorescence inside compared to outside), and not permeable (inside fluorophore intensity was lower compared to outside intensity) membranes (**Figure 4**). Converting M_w to hydrodynamic radius for each fluorophore allows estimating the mesh size of the capsule membrane (**Table 2**).

Selective permeability of protein capsules can be attained during systematic optimization of LbL deposition protocol by using variable concentrations of a prime layer (from 0–6 mg/mL), the concentration of a silk fibroin (from 0.5–2 mg/mL) and the number of deposited layers (from 10–25) until optimal permeability is achieved. In this protocol, optimal permeability between 25–32 nm was achieved with 6 mg/mL of PEI as a prime layer and 20 layers of 1 mg/mL of silk fibroin deposited during LbL assembly (**Figure 4**). This permeability range was ideal for the components of the IVTT system to percolate through the capsule shell. Typically, the largest molecular complexes of any IVTT system are prokaryotic ribosomal units, 30S and 50S, which, when bound by mRNA in a ribosomal complex, can reach up to ~20 nm in size[22]. The structure of the developed microcapsules shells resembles a highly intertwined network of silk fiber layers that are physically crosslinked by β-sheet blocks produced during LbL assembly. This membrane structure is semi-permeable: highly permeable to small molecules (e.g., ions, amino acids, peptides, sugars, etc.) and restricted to large molecules (e.g., high molecular weight proteins, glycoproteins, cells, etc.) that only allows percolation of molecules with a hydrodynamic radius less than 25 nm. Hence, silk fibroin microcapsules with optimal DNA loading and membrane permeability can be used as bioreactor carriers for IVTT activation.

The transcriptional and translational activity of ThyRS and BrocApt design sensors can be tested using commercially available IVTT systems. ThyRS requires translational activation of the reporter gene in the presence of theophylline ligand. Activation of synthetic ThyRS involves several steps to initiate gene expression, including mRNA synthesis, the conformational change of mRNA sequence upon binding to the analyte, release of the ribosome binding site, and the synthesis of the reporter GFPa1 protein. All these steps require free diffusion of the IVTT components through the capsule membrane. The proposed design of DNA-laden silk fibroin microcapsules improved the activation parameters of RNA-regulated sensor designs: Both the expression kinetics and fluorescence output were significantly higher in comparison to the free non-immobilized DNA (**Figure 5A**). The CLSM imaging also confirmed successful GFPa1 gene activation within capsules loaded with DNA plasmids encoding ThyRS sequences (**Figure 5B–D**).

Alternatively, the activation of BrocApt sensor design was carried out in the IVTT system that

supports T7 *E. coli* promoter coupled transcription/translation in the presence of DHFBI-1T dye. The fluorescence output was initiated upon binding the fluorogenic dye to the mRNA sequence. Importantly, the output signal from silk microcapsules was several folds higher compared to non-encapsulated DNA samples of equivalent concentrations (**Figure 6**). Hence, silk fibroin microcapsules can retain the essential functionality of DNA-encoded sensor elements, which can be important for the design of new types of *in vitro* biosensor platforms for rapid and sensitive detection of analytes of interest.

FIGURE LEGENDS:

Figure 1: Plasmid map and sequence of pSALv-RS-GFPa1. (**A**) The plasmid contains theophylline riboswitch (ThyRS) sequence placed upstream of GFPa1 encoding gene under the control of ptac promoter, β-lactamase (bla) encoding gene responsible for resistance to ampicillin. (**B**) The ptac promoter sequence is shown in bold and underlined; theophylline riboswitch sequence is shown in bold italic; GFPa1 encoding sequence is shown in bold; restriction sites sequences are underlined.

Figure 2: Overview of the preparation of microcapsules using the Layer-by-Layer approach. Pristine SiO_2 cores were firstly functionalized with PEI polymer, followed by the sequential deposition of DNA plasmids encoding different sensor designs and silk fibroin layers until the desired number of silk protein layers have been adsorbed. Hollow pristine microcapsules containing various DNA sensor designs can be produced by dissolving sacrificial cores. Activation of each biosensor design encapsulated in the microcapsule can be achieved during IVTT reactions in the presence of corresponding ligands. This figure has been reprinted from Drachuk, I. et al.[21].

Figure 3: Microscopy studies for DNA-loaded microcapsules. (**A**) Cross-sectional 2D and (**B**) Rendered 3D confocal microscopy images of hollow $(SF)_{20}$ microcapsules loaded with DNA plasmids encoding ThyRS (32 DNA copies/capsule) and produced from 6 mg/mL PEI-primed SiO_2 cores. Auto-fluorescence from silk fibroin capsules (DAPI channel, blue) and stained DNA (FITC channel, green) were applied to identify the localization of DNA plasmids and estimate the capsule membrane thickness. Inset in (**A**) represents intensity profiles for DNA and silk fibroin shells across the capsule. Scale bar: 2 μm. Inset in (**B**) represents the intensity profile for silk protein across the capsule shell. Membrane thickness was measured as the length at half intensity peak. Processing of the cross-sectional images and 3D rendering was performed using NIS imaging software on Nikon $C2^+$ system. This figure has been reprinted from Drachuk, I. et al.[21].

Figure 4: Estimation of the membrane permeability for silk microcapsules using the MWCO method. Selective CLSM representative fluorescent images of hollow silk fibroin microcapsules subjected to FITC-Dextran solutions of various M_w (20 μM, diH_2O). Capsules were prepared with a different number of layers and PEI concentrations. An increase in the concentration of a prime layer leads to increased colloidal stability of microcapsules with more permeable shells, while the elimination of the prime layer causes aggregation of capsules with less permeable shell membranes. Scale bar: 5 μm. This figure has been reprinted from Drachuk, I. et al.[21].

Figure 5: **Activation of ThyRS sensor design in silk fibroin microcapsules.** (**A**) Kinetics for GFPa1 expression during ThyRS activation from DNA plasmids loaded into 20-layered SF microcapsules (red-colored lines) and control non-encapsulated DNA (blue-colored lines). From top to bottom, concentrations of DNA in a sample volume (50 µL) were 6.5 ng/µL, 4.5 ng/µL, 2.5 ng/µL, and 0 ng/µL and correspond to the changes in color intensities. (**B**) CLSM images of silk fibroin capsules loaded with 32 DNA copies per capsule. Scale bar: 5 µm. (**C**) The image corresponds to cross-sectional intensity profiles corresponding to image (**B**) across two capsules (white line in **B**). The red line represents silk capsules, and the green line represents GFPa1 expressed in capsules. (**D**) The image represents rendered 3D silk capsules loaded with 32 copies of DNA after incubation in the IVTT system. Green fluorescence corresponds to the GFPa1 signal, and red fluorescence corresponds to fluorescently labeled silk layers. Scale bar: 2 µm. ThyRS activation was performed with theophylline (2 mM, DMSO) during the incubation of microcapsules in the IVTT system (S30 extract). This figure has been reprinted from Drachuk, I. et al.[21].

Figure 6: Activation of BroccApt in silk fibroin microcapsules. Comparison of transcription kinetics was performed for 20-layered silk microcapsules loaded with 30 DNA copies per capsule (red-colored lines) and control non-encapsulated DNA (blue-colored lines). From top to bottom, concentrations of encapsulated DNA in a sample were: 3.6 ng/µL, 2 ng/µL, 1 ng/µL and 0 ng/µL and correspond to the changes in color intensities. Concentrations of non-encapsulated DNA were: 20 ng/µL, 10 ng/µL, 5 ng/µL and 0 ng/µL and correspond to the changes in color intensities. Activation was performed with DHBFI-1T (100 µM, diH_2O) during incubation in the PURE cell-free system. This figure has been reprinted from Drachuk, I. et al.[21].

Table 1: DNA copy number per capsule for each DNA design. The copy number was calculated according to Equation 1 and was correlated to the initial concentration of DNA plasmids, retention affinity of DNA sequences during the LbL deposition process, and the length of DNA plasmids.

Table 2: Physical properties of FITC-dextrans. Hydrodynamic radius for each fluorophore was used to estimate the permeability of hollow silk fibroin microcapsules.

DISCUSSION:

Selectively permeable hydrogel microcapsules loaded with various types of DNA-encoded sensor designs can be prepared following this protocol. One of the distinctive features of the LbL approach is the ability to tailor the complexity of microcapsules during the bottom-up assembly, which usually starts with the adsorption of molecular species on sacrificial templates. By carefully adjusting concentrations of the initial components, pH conditions, and the number of layers, microcapsules with different DNA loading parameters, functionality, and tunable permeability can be prepared[23]. In order to amplify the versatility of the capsules, further functionalization of the shell surface with AuNPs and IgG can be achieved to implement biocompatible sensor carriers for *in vivo* diagnostics. Both of these alternative routes rely on the unique molecular structure of the silk fibroin. In situ reduction of Au^{3+} ions can be accomplished due to the presence of tyrosine

residues (5.3% mol.) capable of reducing metal ions in the presence of an optimal reduction buffer. The conjugation of specific antibodies to the surface of AuNPs-functionalized protein microcapsules can be done *via* the implementation of carbodiimide activation chemistry. Both of these steps require careful development and optimization of the protocol in order to achieve the proper functionality of the biosensor capsules for future applications. For instance, to use these microcapsules as "smart" delivery systems, in which a molecular cargo is delivered upon specific stimuli (like pH or chemical cues), specific properties of these capsules should be characterized and tuned, including delivery efficiency, retention time, route of administration and disease model treatments.

The DNA-loaded microcapsules were characterized by the CLSM technique and fluorescence measurements. However, other characterization methods such as atomic force microscopy (AFM), cryogenic electron tomography (CEM), and direct stochastic reconstruction super-resolution microscopy (dSTORM) can be applied to differentiate specific structures of the microcapsules, including individual fibers, nanodomains, and localization of DNA plasmids[24–26].

The developed protocol highlights the use of silk fibroin biopolymer as a biocompatible network material that preserves the tertiary structure of loaded DNA plasmids. The stability of immobilized DNA sequences within the silk fibroin network occurs via hydrophobic interactions and/or hydrogen bonding, which provide a protective microenvironment against pH inactivation, oxidation or hydrolysis[27]. In addition, the β-crystalline domains of silk fibroin provide a unique mechanical barrier, restricting the movement of entrapped macromolecules, and preventing DNA plasmids from degradation during storage in aqueous solutions.

The semi-permeable nature of silk fibroin microcapsules loaded with DNA templates created unique spatial and physicochemical conditions for the IVTT reactions. Transcriptionally and translationally activated RNA aptamer and riboswitch immobilized in silk fibroin microcapsules were able to produce an output signal that was at least three-fold higher in comparison to free non-immobilized sensors. In addition, the immobilization of DNA templates in microcapsules can significantly enhance the activity of encapsulated sensors beyond the detection limit of non-encapsulated ones. While non-encapsulated sensors had a minimal response at low DNA concentrations, the encapsulated sensors had a very distinct output response, which can be easily titrated to reflect the subtle changes in DNA concentrations. The improved response signal of encapsulated reporters was likely due to unrestricted diffusion of the components of IVTT machinery and reduced mobility of DNA plasmids. Several studies have recognized that the yield of protein synthesis in cell-free reactions is dependent upon the macromolecular environment[28,29]. Immobilization of DNA plasmids into silk network provided an effective confined environment restricting oligonucleotides movement and accelerating transcription/translation mechanism reactions even from several DNA copies[21].

While the LbL method provides a very versatile approach to construct multifunctional assemblies in a controllable manner, the fabrication procedure is relatively time-consuming and typically requires processing adjustments to scale up the microcapsules yield. Another consideration in making biomolecule-based microcapsules is the compatibility of any given system with the

requirement for the core dissolution after LbL deposition is completed. So far, to produce homogeneous in size and robust hollow silk-based DNA-laden microcapsules, the shells were deposited on sacrificial silica (SiO_2) core templates, which required subsequent removal by hydrofluoric (HF) acid etching. Nor HF handling or etching are considered biocompatible processes, limiting their widespread use in practical applications. The alternative to SiO_2 inorganic colloidal templates, carbonate cores are typically inert in forming complexes with polymer layers and can be dissolved under mild conditions using ethylenediaminetetraacetic acid (EDTA). However, adjusting sacrificial cores may affect the deposition properties of multilayers and the integrity of the shell structure, which requires further optimization of the protocol.

In summary, the current protocol allows the preparation of silk-based DNA-laden microcapsules with different sensor designs. The combination of a confined microenvironment provided by the LbL method and the use of silk fibroin as a biocompatible material improved the sensing properties of encapsulated DNA. With the rapid development of fluorogenic RNA aptamer technology, the potential use of DNA-laden silk microcapsules can be extended to multiplexed *in vitro* diagnostics. Recently, several variations of RNA-based fluorescent aptamers have emerged as powerful background-free technology for imaging RNA in live cells with high signal-to-noise ratio sensitivity[30,31]. By applying synthetic RNA nanotechnology to design artificial RNA aptamers, the fluorogenic properties of aptamers can be harnessed to detect specific ligands of interest. This technology will be specifically valuable to monitor biomarkers of interest in different formats, including point-of-use paper-based sensors, hydrogel-based patches for sweat or interstitial fluid, and implantable materials.

ACKNOWLEDGMENTS:

This work was supported by LRIR 16RH3003J grant from the Air Force Office of Scientific Research, as well as the Synthetic Biology for Military Environments Applied Research for the Advancement of S&T Priorities (ARAP) program of the U.S. Office of the Under Secretary of Defense for Research and Engineering.

The plasmid vector sequence for ThyRS (pSALv-RS-GFPa1, 3.4 kb) was generously provided by Dr. J. Gallivan. Silkworm cocoons from *Bombyx mori* were generously donated by Dr. D.L. Kaplan from Tufts University, MA.

DISCLOSURES:

The authors have nothing to disclose.

REFERENCES:

1. Slomovic, S., Pardee, K., Collins, J. J. Synthetic biology devices for in vitro and in vivo diagnostics. *Proceedings of the National Academy of Sciences of the United States of America*. **112** (47), 14429–14435 (2015).
2. Harbaugh, S. V., Goodson, M. S., Dillon, K., Zabarnick, S., Kelley-Loughnane, N. Riboswitch-based reversible dual-color sensor. *ACS Synthetic Biology* **6** (5), 766–781 (2017).
3. König, H., Frank, D., Heil, R., Coenen, C. Synthetic genomics and synthetic biology applications between hopes and concerns. *Current Genomics*. **14** (1), 11–24 (2013).
4. Silverman, A. D., Karim, A. S., Jewett, M. C. Cell-free gene expression: An expanded

repertoire of applications. *Nature Reviews Genetics.* **21**, 151–170 (2020).
5. Chushak, Y. et al. Characterization of synthetic riboswitch in cell-free protein expression systems. *RNA Biology*, 1–12 (2021).
6. Cole, S. D., et al. Quantification of interlaboratory cell-free protein synthesis variability. *ACS Synthetic Biology.* **8** (9), 2080–2091 (2019).
7. Thavarajah, W. et al. Point-of-use detection of environmental fluoride via a cell-free riboswitch-based biosensor. *ACS Synthetic Biology.* **9** (1), 10−18 (2020).
8. Gräwe, A., et al. A paper-based, cell-free biosensor system for the detection of heavy metals and date rape drugs. *PLoS One* **14** (3), e0210940 (2019).
9. Lin, X. et al. Portable environment-signal detection biosensors with cell-free synthetic biosystems. *RSC Advances.* **10** (64), 39261–39265 (2020).
10. Caschera, F., Lee, J. W., Ho, K. K. Y., Liu A. P., Jewett, M. C. Cell-free compartmentalized protein synthesis inside double emulsion templated liposomes with in vitro synthesized and assembled ribosomes. *Chemical Communications.* **52** (31), 5467–5469 (2016).
11. Niederholtmeyer, H., Chaggan, C., Devaraj, N. K. Communication and quorum sensing in non-living mimics of eukaryotic cells. *Nature Communications.* **9**, e5027 (2018).
12. Timin, A. S., Gould, D. J.; Sukhorukov. G. B. Multi-layer microcapsules: Fresh insights and new applications. *Expert Opinion on Drug Delivery.* **14** (5), 583–587 (2017).
13. Bomati, E. K., Haley, J. E., Noel, J. P., Deheyn, D. D. Spectral and structural comparison between bright and dim green fluorescent proteins in Amphioxus. *Scientific Reports*. **4**, e5469 (2014).
14. Frey B. *Amplification of Genomic DNA by PCR*. In: Reischl U. (eds) *Molecular Diagnosis of Infectious Diseases*. *Methods in Molecular Medicine*™, **13**, 143–156. Humana Press, Totowa, NJ (1998).
15. Lee, P.Y., Costumbrado, J., Hsu, C.-Y., Kim, Y.H. Agarose gel electrophoresis for the separation of DNA fragments. *Journal of Visualized Experiments*. **62**, e3923, (2012).
16. Zhou, Y. et al. Rapid regeneration and reuse of silica columns from PCR purification and gel extraction kits. *Scientific Reports.* **8**, 12870 (2018).
17. Kostylev, M., Otwell, A. E., Richardson, R. E., Suzuki, Y. Cloning should be simple: *Escherichia coli* DH5α-mediated assembly of multiple DNA fragments with short end homologies. *PLoS One*. **10** (9), e0137466 (2015).
18. Rockwood, D. N. et al. Materials fabrication from *Bombyx mori* silk fibroin. *Nature Protocols.* **6** (10), 1612–1631 (2011).
19. Drachuk I. et al. Silk macromolecules with amino acid-Poly(Ethylene Glycol) grafts for controlling layer-by-layer encapsulation and aggregation of recombinant bacterial cells. *ACS Nano.* **9** (2), 1219–1235 (2015).
20. Antipov, A. A., Sukhorukov, G. B. Polyelectrolyte multilayer capsules as vehicles with tunable permeability. *Advances in Colloid and Interface Science.* **111** (1–2), 49–61 (2004).
21. Drachuk, I., Harbaugh, S., Chávez, J. L., Kelley-Loughnane, N. Improving the activity of DNA-encoded sensing elements through confinement in silk microcapsules. *ACS Applied Materials & Interfaces.* **12** (43), 48329–48339 (2020).
22. Melnikov, S., Ben-Shem, A., Garreau de Loubresse, N., Jenner, L., Yusupova, G., Yusupov, M. Structural basis for the inhibition of the eukaryotic ribosome. *Nature Structural & Molecular Biology.* **19** (6), 560–567 (2012).

23. Zhao, S., et al. The future of layer-by-layer assembly: A tribute to ACS Nano associate editor Helmuth Möhwald. *ACS Nano.* **13** (6), 6151–6169 (2019).
24. Main, K. H. S., Provan, J. I., Haynes, P. J., Wells, G., Hartley, J. A., Pyne, A. L. B. Atomic force microscopy—A tool for structural and translational DNA research. *APL Bioengineering*. **5**, 031504 (2021).
25. Riera, R., Feiner-Gracia, N., Fornaguera, C., Cascante, A., Borrós, S., Albertazzi, L. Tracking the DNA complexation state of pBAE polyplexes in cells with super resolution microscopy. *Nanoscale*. **11** (38), 17869-17877 (2019).
26. Bilokapic, S., Strauss, M., Halic, M. Cryo-EM of nucleosome core particle interactions in trans. *Scientific Reports*. **8**, 7046 (2018).
27. Pritchard, E. M., Dennis, P. B., Omenetto, F., Naik, R. R., Kaplan, D. L. Physical and chemical aspects of stabilization of compounds in silk. *Biopolymers.* **97** (6) 479–498 (2012).
28. Fritz, B. R., Jamil, O. K., Jewett, M. C. Implications of macromolecular crowding and reducing conditions for in vitro ribosome construction. *Nucleic Acids Research.* **43** (9), 4774–4784 (2015).
29. Ge, X., Luo, D., Xu, J. Cell-free protein expression under macromolecular crowding conditions. *PLoS One.* **6** (12), e28707 (2011).
30. Cawte, A. D., Unrau, P. J., Rueda, D. S. Live cell imaging of single RNA molecules with fluorogenic mango II arrays. *Nature Comm*unications. **11**, e1283 (2020).
31. Chen, X. et al. Visualizing RNA dynamics in live cells with bright and stable fluorescent RNAs. *Nature Biotechnology.* **37** (11), 1287–1293 (2019).

Figure 1

Click here to access/download;Figure;Figure1.docx

A

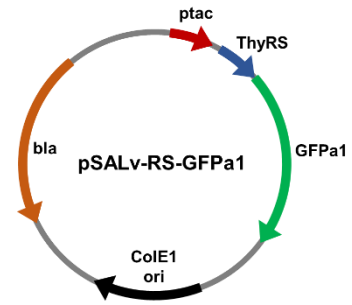

B

TCGCGCGTTTCGGTGATGACGGTGAAAACCTCTGACACATGCAGCTCCCGGAGACGGTCACAGCTTGTCTGTAAGCGGATGCCGGGAGCAGACAAGCCCGT
CAGGGCGCGTCAGCGGGTGTTGGCGGGTGTCGGGGCTGGCTTAACTATGCGGCATCAGAGCAGATTGTACTGAGAGTGCACCATATGCGGTGTGAAATACC
GCACAGATGCGTAAGGAGAAAATACCGCATCAGGCGCCATTCGCCATTCAGGCTGCGCAACTGTTGGGAAGGGCGATCGGTGCGGGCCTCTTCGCTATTACG
CCAGCTGGCGAAAGGGGGATGTGCTGCAAGGCGATTAAGTTGGGTAACGCCAGGGTTTTCCCAGTCACGACGTTGTAAAACGACGGCCAGTGCCAAACTTG
CATGCCTGCAGGTCGACTCTAGT**GAGCTGTTGACAATTAATCATCGGCTCGTATAATGTGTGG**GCTAACAAGTCTAGCGAACCGCACTTAATACGACTCACTAT
AGGTACCG***GTGATACCAGCATCGTCTTGATGCCCTTGGCAGCACCCTGCTAAGGTAACAACAAG***ATGCCTCTGCCCGCAACCCACGACATCCACCTTCACG
GCTCCATCAACGGCCACGAGTTCGACATGGTGGGGGGAGGAAAAGGCGACCCGAACGCCGGCTCGCTGGTGACCACAGCGAAATCCACCAAGGGTGCC
CTGAAGTTCTCTCCCTACTTGATGATCCCCCACCTCGGGTACGGGTACTACCAGTACCTCCCCTACCCGGACGGACCCTCGCCTTTCCAGGTCTCCATGTTG
GAAGGATCGGGGTATGCAGTCTACCGCGTGTTCGACTTTGAAGACGGAGGCAAGCTGTCTACCGAGTTTAAGTACTCCTACGAGGGTTCCCATATCAAGGC
CGACATGAAGCTGATGGGAAGCGGTTTCCCTGACGACGGCCCAGTCATGACCAGCCAGATTGTCGACCAGGACGGCTGCGTGTCCAAGAAGACGTATCTT
AACAACAACACCATCGTGGACAGCTTCGACTGGAGTTACAACCTGCAGAATGGGAAGCGCTACAGGGCCCGAGTGTCGAGCCACTACATCTTCGACAAGC
CCTTTTCAGCCGATCTCATGAAGAAGCAGCCGGTCTTCGTTTACCGCAAGTGCCACGTGAAGGCTACCAAGACCGAAGTCACCCTGGACGAGAGGGAGAA
GGCGTTCTACGAGCTGGCTTAAGCTGAGCGCCGGTCGCTACCATTACCAGTTGGTCTGGTGTCAAAAATAATAATAACCGGGCAGGCCATGTCTGCCCGTATTT
CGCGTAAGGAAATCCATTATGTACTATTTCTGCATTAATGAATCGGCCAACGCGCGGGGAGAGGCGGTTTGCGTATTGGGCGCTCTTCCGCTTCCTCGCTCACT
GACTCGCTGCGCTCGGTCGTTCGGCTGCGGCGAGCGGTATCAGCTCACTCAAAGGCGGTAATACGGTTATCCACAGAATCAGGGGATAACGCAGGAAAGAAC
ATGTGAGCAAAAGGCCAGCAAAAGGCCAGGAACCGTAAAAAGGCCGCGTTGCTGGCGTTTTTCCATAGGCTCCGCCCCCCTGACGAGCATCACAAAAATCGA
CGCTCAAGTCAGAGGTGGCGAAACCCGACAGGACTATAAAGATACCAGGCGTTTCCCCCTGGAAGCTCCCTCGTGCGCTCTCCTGTTCCGACCCTGCCGCTT
ACCGGATACCTGTCCGCCTTTCTCCCTTCGGGAAGCGTGGCGCTTTCTCATAGCTCACGCTGTAGGTATCTCAGTTCGGTGTAGGTCGTTCGCTCCAAGCTGG
GCTGTGTGCACGAACCCCCCGTTCAGCCCGACCGCTGCGCCTTATCCGGTAACTATCGTCTTGAGTCCAACCCGGTAAGACACGACTTATCGCCACTGGCAG
CAGCCACTGGTAACAGGATTAGCAGAGCGAGGTATGTAGGCGGTGCTACAGAGTTCTTGAAGTGGTGGCCTAACTACGGCTACACTAGAAGGACAGTATTTGG
TATCTGCGCTCTGCTGAAGCCAGTTACCTTCGGAAAAAGAGTTGGTAGCTCTTGATCCGGCAAACAAACCACCGCTGGTAGCGGTGGTTTTTTTGTTTGCAAG
CAGCAGATTACGCGCAGAAAAAAAGGATCTCAAGAAGATCCTTTGATCTTTTCTACGGGGTCTGACGCTCAGTGGAACGAAAACTCACGTTAAGGGATTTTGGT
CATGAGATTATCAAAAAGGATCTTCACCTAGATCCTTTTAAATTAAAAATGAAGTTTTAAATCAATCTAAAGTATATATGAGTAAACTTGGTCTGACAGTTACCAATG
CTTAATCAGTGAGGCACCTATCTCAGCGATCTGTCTATTTCGTTCATCCATAGTTGCCTGACTCCCCGTCGTGTAGATAACTACGATACGGGAGGGCTTACCATC
TGGCCCCAGTGCTGCAATGATACCGCGAGACCCACGCTCACCGGCTCCAGATTTATCAGCAATAAACCAGCCAGCCGGAAGGGCCGAGCGCAGAAGTGGTC
CTGCAACTTTATCCGCCTCCATCCAGTCTATTAATTGTTGCCGGGAAGCTAGAGTAAGTAGTTCGCCAGTTAATAGTTTGCGCAACGTTGTTGCCATTGCTACAG
GCATCGTGGTGTCACGCTCGTCGTTTGGTATGGCTTCATTCAGCTCCGGTTCCCAACGATCAAGGCGAGTTACATGATCCCCCATGTTGTGCAAAAAAGCGGT
TAGCTCCTTCGGTCCTCCGATCGTTGTCAGAAGTAAGTTGGCCGCAGTGTTATCACTCATGGTTATGGCAGCACTGCATAATTCTCTTACTGTCATGCCATCCGT
AAGATGCTTTTCTGTGACTGGTGAGTACTCAACCAAGTCATTCTGAGAATAGTGTATGCGGCGACCGAGTTGCTCTTGCCCGGCGTCAATACGGGATAATACCG
CGCCACATAGCAGAACTTTAAAAGTGCTCATCATTGGAAAACGTTCTTCGGGGCGAAAACTCTCAAGGATCTTACCGCTGTTGAGATCCAGTTCGATGTAACCC
ACTCGTGCACCCAACTGATCTTCAGCATCTTTTACTTTCACCAGCGTTTCTGGGTGAGCAAAAACAGGAAGGCAAAATGCCGCAAAAAAGGGAATAAGGGCGA
CACGGAAATGTTGAATACTCATACTCTTCCTTTTTCAATATTATTGAAGCATTTATCAGGGTTATTGTCTCATGAGCGGATACATATTTGAATGTATTTAGAAAAATAA
ACAAATAGGGGTTCCGCGCACATTTCCCCGAAAAGTGCCACCTGACGTCTAAGAAACCATTATTATCATGACATTAACCTATAAAAATAGGCGTATCACGAGGCC
CTTTCGTC

Figure 2

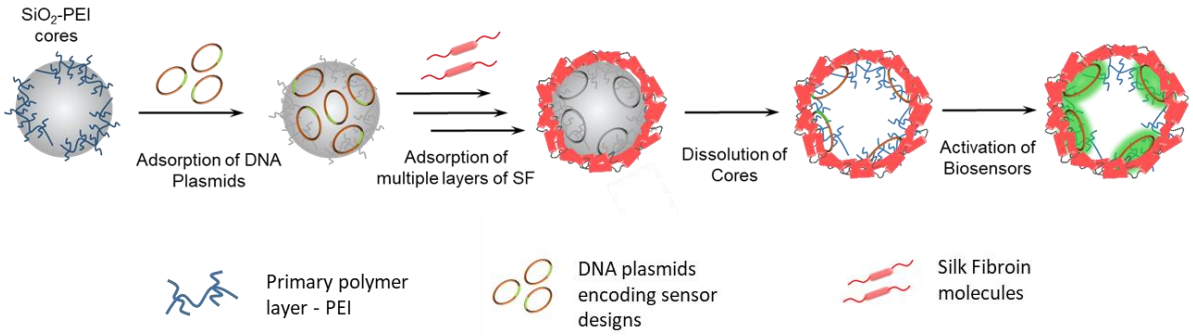

Figure 3

Click here to access/download;Figure;Figure3.docx

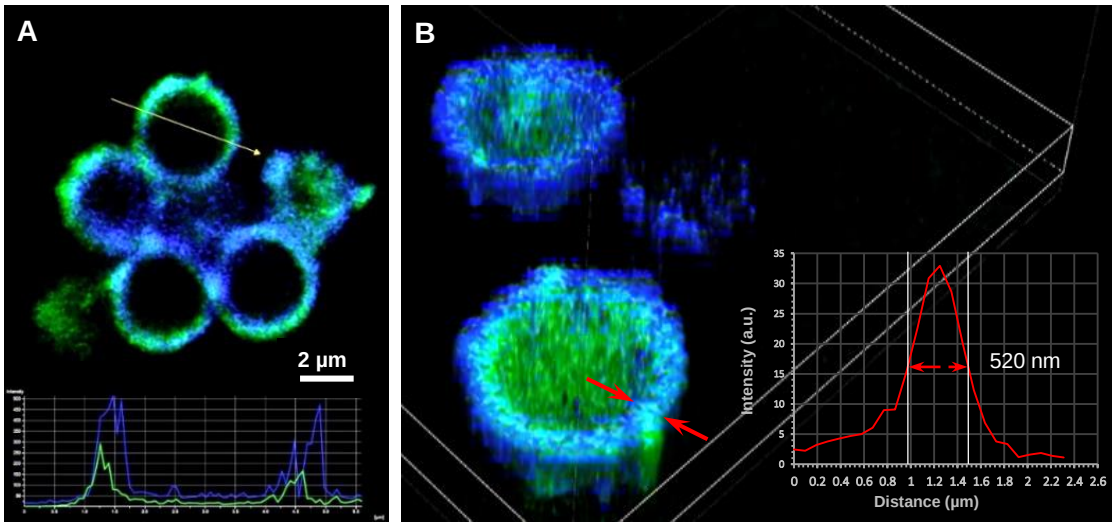

Figure 4

Click here to access/download;Figure;Figure4.docx

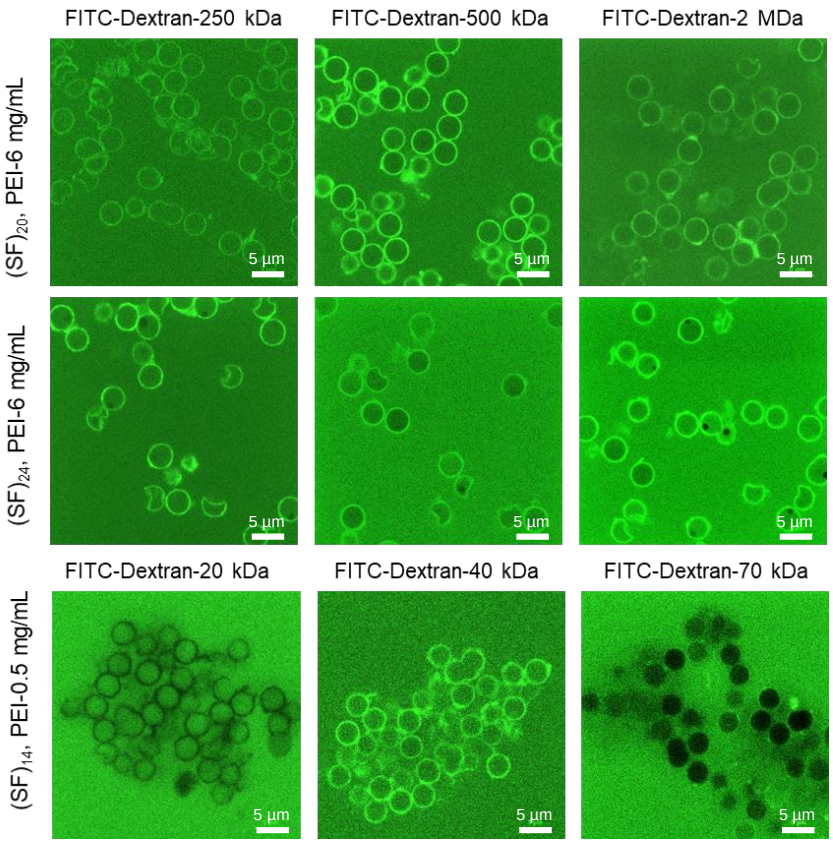

Figure 5

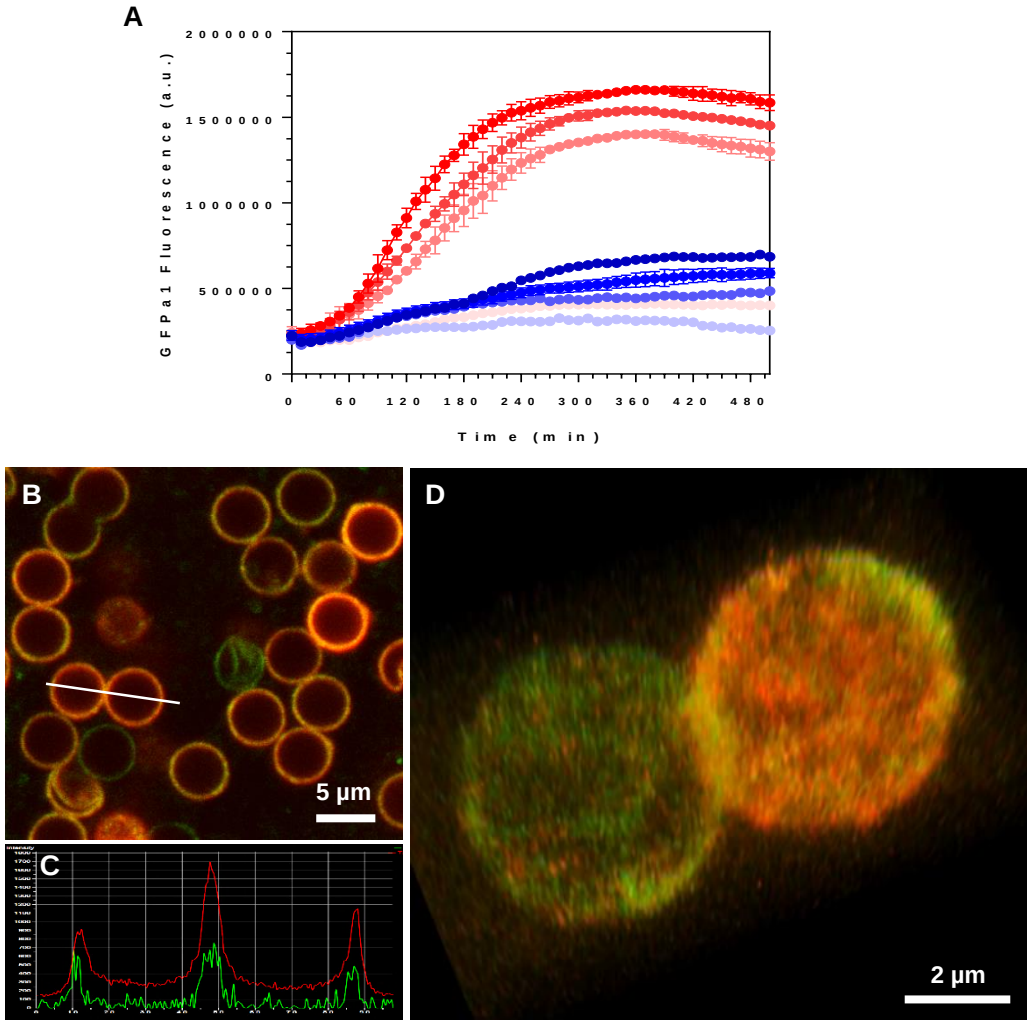

Figure 6

Click here to access/download;Figure;Figure6.docx

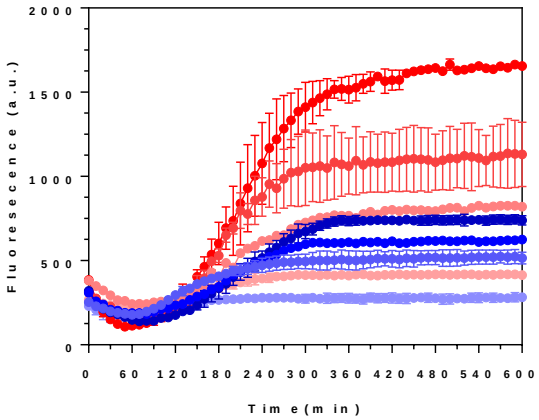

Table 1

DNA Sensor Design	Initial DNA Concentration (ng/µL)	Number of DNA copies per capsule (DNA/capsule)
ThyRS	50	16
	100	32
	150	48
	200	64
BrocApt	50	10
	100	20
	150	30
	200	40

Table 2

Mw of FITC-Dextran (kDa)	Hydrodynamic Radius (nm)
4	1.4
20	3.3
40	4.5
70	6
150	8.5
250	10
500	14
2,000	18

Response to the Reviewers' and Editor Comments

We appreciate the time and effort the Reviewers and Editor took to address the issues in our manuscript. Below are the responses to Reviewers comments:

Reviewer 1.

1. We appreciate the Reviewer's comment on adding other characterization methods (SEM, AFM, TEM) to visualize microcapsules. However, we would like to point out that the main focus of our paper was on developing a protocol on preparing DNA-laden silk fibroin microcapsules, and demonstrating that DNA sensor designs can be activated with corresponding ligands. Hence, the current CLSM technique and fluorescence-based multi-well plate reader were the main characterization techniques that could provide ample information to confirm the activity of DNA as well as other properties of microcapsules.
2. The conjugation of IgG to the capsule shell and *in-situ* synthesis of AuNPs to produce multifunctional capsules are optional approaches. We removed the second route to produce multifunctional assemblies from the Scheme to lessen the confusion and focus on the main objective of the protocol – preparation of *in vitro* Sensor designs.
3. We would like to reiterate that the focus of our paper was to develop a protocol of preparing DNA-laden silk fibroin microcapsules with various activation designs. While the following in vivo characteristics: delivery efficiency, retention time, route of administration and disease model of treatments sound as interesting approaches for characterization, we did not use our systems in animal/human models. This will be an excellent follow-up experiments for the future scientific papers.

Reviewer 2.

1. The mistake in Figure 3B was corrected. Thank you for pointing that out.
2. The Scheme in Figure 2 was cleaned. We removed the alternative route 2 for making multifunctional microcapsules. We also added legends to make the scheme look coherent.
3. The scale bars were added to the figure. Thank you for pointing this out.

Editorial Comments:

1. We addressed the abbreviations, and proofread the manuscript.
2. Email addresses for each author were added.
3. References were formatted accordingly.
4. The text was revised to avoid overlapping with our published paper.
5. The trademarks and registered symbols were removed from the main paper and all reagents/materials/supplies have been moved to Materials and Reagents Table.
6. Materials source was moved to Acknowledgements section.
7. The manuscript was revised to avoid the use of personal pronouns.
8. The text was also revised using imperative tense.

9. We revised the protocol to include every detail necessary to perform the step. We believe each step was sufficiently described. For steps that are not essential for the developed protocol, necessary references were added.
10. Steps in the protocol were highlighted for filming.
11. Titles and Figure Legends were removed from the figures, and moved to the Section after the Representative Results.
12. Scale bars were added to the Figures, as well as the scale definition was added to the Figure Legend.
13. Tables were removed from the Figures Section. Table names and the legends were moved to the appropriate section.
14. Limitations of the current protocol were added to the Discussion section.
15. References were edited according to the Journal's format. We included the article volume, issue number and pages, except for electronic versions of the journals, where no pages of the article were provided, where we incorporated only the article number. Examples, *Nature Communications*, *PLoS One*.

Improving the Activity of DNA-Encoded Sensing Elements through Confinement in Silk Microcapsules

Author: Irina Drachuk, Svetlana Harbaugh, Jorge L. Chávez, et al
Publication: Applied Materials
Publisher: American Chemical Society
Date: Oct 1, 2020

PERMISSION/LICENSE IS GRANTED FOR YOUR ORDER AT NO CHARGE

This type of permission/license, instead of the standard Terms & Conditions, is sent to you because no fee is being charged for your order. Please note the following:

- Permission is granted for your request in both print and electronic formats, and translations.
- If figures and/or tables were requested, they may be adapted or used in part.
- Please print this page for your records and send a copy of it to your publisher/graduate school.
- Appropriate credit for the requested material should be given as follows: "Reprinted (adapted) with permission from (COMPLETE REFERENCE CITATION). Copyright (YEAR) American Chemical Society." Insert appropriate information in place of the capitalized words.
- One-time permission is granted only for the use specified in your request. No additional uses are granted (such as derivative works or other editions). For any other uses, please submit a new request.

If credit is given to another source for the material you requested, permission must be obtained from that source.

BACK CLOSE WINDOW